

# Comparative Structural Integrity of Miura-Ori and Flasher Origami Patterns for Deployable Solar Panels

Aruzhan Muratbekova

Haileybury Almaty, Al-Farabi Avenue 112, Almaty, 050040, Kazakhstan; muraaruzhan@gmail.com  
Mentor: S. Bullock

**ABSTRACT:** With the introduction of origami folding patterns into deployable structures in space in the mid-2000s, the field of aerospace engineering experienced an innovative breakthrough with new benefits. The advantages of using origami principles in deployable structures are undeniable; from reduced weight and costs to enhanced functionality, origami in spacecraft has significantly increased efficiency. The deployment of solar panels, specifically, is heavily dependent on utilizing origami-inspired structures to maximize the surface area for energy absorption while minimizing the storage volume. For the better performance of solar panel deployment, the origami structure must have high structural integrity to withstand the space environment and external impacts. This paper presents two folding patterns, comparing their structural integrity: Miura-Ori and Flasher origami folds. The study focused on the comparison and evaluation, specifically assessing their strength and structural integrity through physical experimentation using smaller-scale Mylar and Flasher models. As a result of physical testing, the Flasher outperformed Miura-Ori by 16% in terms of strength, indicating it to be a more impact-resistant origami structure. It is hypothesized that the rotational symmetry of Flasher distributes compressive stress more evenly, yielding a higher peak load than the parallelogram tessellation of Miura-Ori.

**KEYWORDS:** Engineering Mechanics, Aerospace and Aeronautical Engineering, Solar Panels, Miura-Ori, Flasher.

## ■ Introduction

Solar cells (SCs) are single units that convert solar energy into electricity using the photovoltaic effect. Solar panels (SPs) are structures made up of multiple SCs to convert this energy on a larger scale. SPs are widely used and reliable for energy generation in aerospace applications, where photovoltaic devices can provide an uninterrupted and stable power supply.<sup>1</sup> Over the past 50 years since 1970, the power conversion efficiency of photovoltaic technologies has increased, reaching a mean value of 28.95% for different SC materials.<sup>1</sup> Considering the value of solar energy and the effective use of photovoltaic abilities, SPs have become one of the most valuable and widely used energy-generating technologies in spacecraft (including artificial satellites as well as exploration technologies), serving as the primary energy source for various space missions.<sup>2</sup> And one of the methods used for SPs to absorb sun energy and convert it to electricity is photovoltaics.<sup>3</sup>

Among the power generation systems, the photovoltaic cells remain a stronger option, specifically for long-term space missions, in contrast to nonrechargeable batteries and fuel cells.<sup>1</sup> The advantages and reasons why the use of SPs has become more widespread in spacecraft energy-generating systems include the following: Sustainability and independence from finite resources, Energy storage in advance, No refuelling necessity, Lightweight, Low cost, High availability, and stock.<sup>4</sup> All of these advantages maximize the convenience of using SPs in spacecraft. However, they do not completely exclude possible problems caused by the size of SPs in larger spacecraft, where more SCs are used to provide a bigger surface area for solar energy intake.<sup>4</sup> As a result, many designs struggle with

limited power generation capabilities, leaving fewer opportunities for larger spacecraft maintenance.<sup>4</sup> This issue creates a need to develop simplified deployable mechanisms to create more compact designs, easing the launch of spacecraft.

These problems have been addressed by a Japanese paper-folding technique, origami, which has been implemented in space engineering as a promising approach to reduce the challenges associated with SP design.<sup>4</sup> The concept of using origami in space missions allows for the development of solar panels that can unfold or expand upon deployment, providing a larger surface area for energy collection.<sup>1</sup> Origami-inspired techniques in space engineering help alleviate multiple negative aspects of using large SPs. Consequently, there are several reasons why origami brings additional advantages to SPs, including higher cost efficiency, improved space and weight efficiency, reduced friction and wear, and increased precision due to more options for scalability.<sup>4,5</sup>

Despite the advantages that origami-based aerospace designs provide, solar panels are prone to structural failures due to the harsh conditions of space, including external impacts such as micrometeoroid impacts or space debris.<sup>1</sup> This is even more applicable in the case of larger surface area SPs, making them much more vulnerable and requiring them to withstand physical damage.<sup>1</sup> Structural integrity concerns can be addressed by designing specific origami patterns to distribute stress more evenly and better absorb external impacts.<sup>6</sup>

There are numerous origami patterns used for SP deployment. The Miura and Flasher designs stand out as the most common configurations utilized in SPs.<sup>4</sup> Researchers at Brigham Young University have indicated that engineers and

scientists focus on the following properties of origami: 1) Stowability, 2) Portability, 3) Deployability, 4) Fewer components, 5) Manufacturability, 6) Lower volume and mass, and 7) Ease of miniaturization and assembly.<sup>4,5</sup> While meeting all of these requirements, the Miura and Flasher folding designs are also examples of rigid origami consisting of rigid folds. Rigid folds have surfaces surrounded by crease lines, and the ones that do not bend. Both Flasher and Miura satisfy the implementation of rigid origami without deformation due to flexible crease lines.<sup>4</sup> Each rigid section of origami can pivot around the creases, allowing these creases to be viewed as revolute joints in mechanical design. Likewise, the entire crease pattern with a single vertex can be considered a spherical linkage. This is because, when the paper is folded into a 3-D shape, the intersections of the creases and edges maintain equal distances from the vertex.<sup>4</sup> As this paper focuses on the structural integrity of origami folds, it is essential to examine each origami pattern's mechanical properties in detail.

### Miura-Ori

One of the rigidly folded types, Miura-Ori, is an origami pattern consisting of several single units that consist of four identical parallelograms surrounding vertices, and consisting of a single mountain and valley creases. This single unit of four quadrangle plates repeats throughout the pattern, forming a tessellation, as shown in Figure 1.<sup>7</sup> It consists of interchanging, repeating mountain and valley creases in a sequence.<sup>7</sup> One unit of Miura-Ori has a single vertex angle ( $\alpha$ ) and a single span length ( $a$ ), as well as the second span length ( $b$ ).

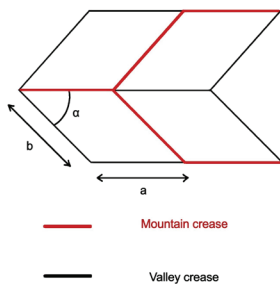


**Figure 1:** Single Miura-Ori unit showing a mountain and valley creases, as well as span lengths  $a$  and  $b$  along with vertex angle  $\alpha$ .

Due to its characteristics, this pattern could be arranged for various performance purposes, for example, by adding another interchanging angle ( $\beta$ ) or varying the span length.<sup>7</sup> There are also multiple variations in the design of Miura-Ori where both the angles and span length are changed to different quantities, making its structure fold in different ways while still retaining its original form, for example, by forming more of an arch figure.<sup>7</sup> To keep this research as fair as possible, the most common version of the Miura-Ori design has been kept for the physical testing.

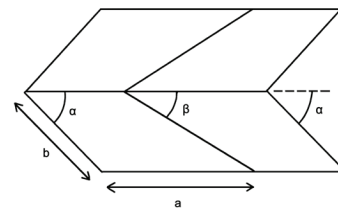


**Figure 2:** Single Miura-Ori unit with the introduction of angle  $\beta$ . All of the other dimensions shown are kept the same.

Figure 2 shows an example of another Miura-Ori single cell variation by introducing a new angle beta to the system. One of the most important mechanical features of Miura-Ori is the degree of freedom determined by the angle  $\theta$ .<sup>8</sup> This is the angle between two faces and is responsible for the energy absorption capabilities and in-plane behaviors.<sup>8</sup> This tessellation pattern is widely used for engineering purposes due to its high stiffness-to-weight ratio and successful energy absorption performance, making Miura-Ori an extremely high stress-absorbing origami pattern.<sup>8</sup> Dihedral angle is the angle between the 2 creases within an origami that determines its strength. When span lengths  $a$ ,  $b$ , and angle  $\alpha$  are constant, the unit performance depends on the dihedral angle  $\theta$ , as shown in Figure 3. It is also essential to mention that the span lengths  $a$  and  $b$  would be equal for this to work.<sup>8</sup> Because an optimal angle theta relies on the value of alpha, the optimal value for both will be used.<sup>9</sup>

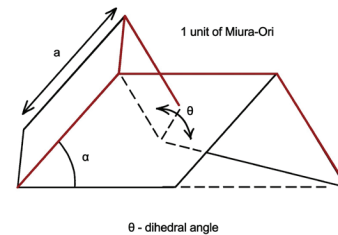


**Figure 3:** Showing a single Miura-Ori unit with the introduction of angle  $\theta$  in a three-dimensional diagram.

Looking more specifically at the architectural role of Miura-Ori, its self-locking feature enables the opportunity for this tessellation to be used in terms of mechanics and structure, where it can form structures that resemble arches and shells when modified.<sup>10</sup> It is also shown that Miura-Ori's pattern parts could be removed without causing any changes in its origami behaviour, showing its advantages for architectural modifications.<sup>10</sup> For the physical testing part, the following dimensions were considered as optimal for the dihedral angle:  $\theta=50^\circ$ .<sup>10</sup>

### Flasher:

Flasher is another type of rigid origami, similar to Miura-Ori; however, their fundamental structures differ. Origami Flashers have a cyclic symmetry within their structure, with the number of edges of the central regular polygon determining the number of identical sectors.<sup>11</sup> This rotationally symmetric set of creases is folded around the polygonal cylinder in the center.<sup>12</sup> The edges of the hub(central polygon) and the folds where they meet are considered valley folds. Lines that divide these valley folds are also added, creating the mountain folds

in between. The creases in the Flasher and the overall folding direction can only face clockwise or counterclockwise.<sup>11</sup>

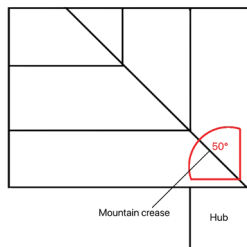


**Figure 4:** A fragment of the square Flasher showing the fold line at  $50^\circ$  for the mountain crease.

In Figure 4, the most basic Flasher pattern used is shown; the model is directed clockwise and has a pattern with the square central hub. Like any rigid origami, Flasher has alternating sequences of mountain and valley creases. To demonstrate this, Figure 3 below is shown.

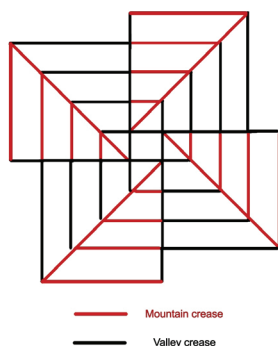


**Figure 5:** Basic expanded Flasher model with different colours representing their corresponding mountain and valley creases.

Figure 5 illustrates the origami patterns of planar origami flashers considering four different central hubs. The red lines and black lines represent the mountain creases and valley creases, respectively.<sup>11</sup> Mechanical behavior is strongly dependent on folding dihedral angles at mountain and valley creases. These angles determine whether the pattern collapses into a flattened disk or cones, its deployment stiffness, and final unloaded shape.<sup>13</sup> Dihedral fold angle is directly linked to deployment path, strain energy, and mechanical fatigue performance, making it the most important factor in deciding the overall structural integrity of the origami Flasher model.<sup>14</sup> For the optimal performance of the flasher unit, it is essential to keep the dihedral angle  $\theta$  at a value of  $50^\circ$ .<sup>14</sup>

There are numerous studies assessing each origami folding pattern in terms of their structural integrity and dynamic mechanical properties with different acute angles in quasi-static and fully static conditions, where the optimal acute angles at peaks and compression distances for the highest energy absorption have been investigated.<sup>15</sup> Taking this into account, this paper aims to produce a comparison between the two structures and set up its own testing method to evaluate which origami pattern between the two origami patterns would be stronger. This gap is significant because in space missions with the use of SPs, where the potential hazards are more prominent, the factor of structural integrity would play a crucial role

in suppressing the negative effects of collisions. Hence, the choice of the origami pattern used for deployment would play a role in that, deciding the goal of this paper to compare the 2 most common patterns in terms of their ability to withstand external impacts. By analysing each folding pattern's performance in load and stretch testing, this study allows engineers to choose the strongest origami folding pattern for SPs. The significance of this study lies in its potential to use the design of SPs in spacecraft for missions with a high risk of external impact, ultimately contributing to more efficient and sustainable space exploration. The hypothesis guiding this research is that the Miura and Flasher origami patterns will demonstrate varying degrees of structural integrity in terms of strength and flexibility, impacting their effectiveness in SP applications in space.

## ■ Methods

This research aims to evaluate the structural integrity of deployable solar panels designed using Miura and Flasher origami patterns. These patterns were chosen due to their established effectiveness in optimizing space utilization and enhancing deployable structures in aerospace applications.<sup>4</sup> The methodology encompasses model design and fabrication, experimental setup, and a comprehensive assessment of performance metrics, including load-bearing capacity.

### *Design and Fabrication:*

Models of deployable SPs will be constructed for the physical tests, where each model will be measuring 15 cm x 15 cm in their deployed state, representing a smaller scale of typical solar panels used in space missions. Each origami pattern will consist of five identical models for each origami folding type, resulting in a total of ten models. It has been decided that at least 5 models will be tested for each origami pattern to collect the mean and ensure the results are as reliable as possible with the inclusion of random error. In the experiment setup, a sample size of 5 has been considered a reasonable number to investigate the connection. The Miura origami fold will consist of 2 x 2 cells, like in Figure 6. Flasher origami fold will be made from a 7 x 7 square base with a square quadrilateral base, resulting in 4 clockwise vertices, like in Figure 6 as well. The paper prototypes could be seen and compared to the Mylar Miura and Flasher in the images below in Figure 7. And Figure 8.

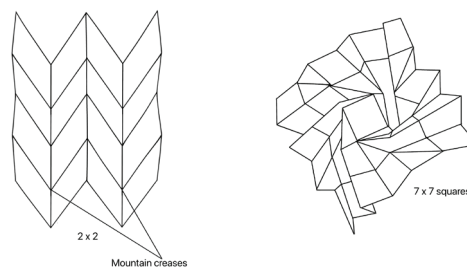


**Figure 6:** Upper view of the Miura (on the left) and Flasher (on the right) origami folds in a 2-D diagram.

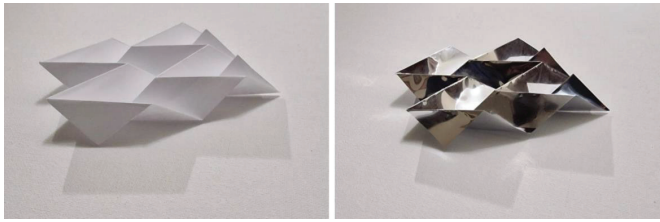


**Figure 7:** Paper Miura Fold on the left and Mylar Miura Fold on the right.

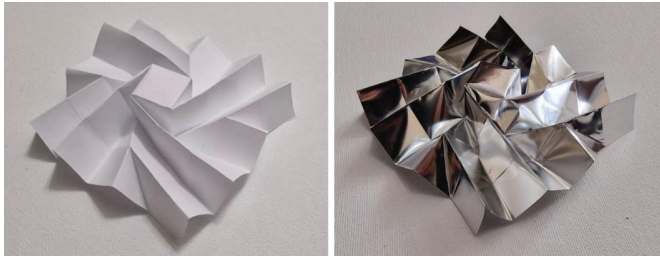


**Figure 8:** Paper Flasher Fold on the left and Mylar Flasher Fold on the right.

There are proven to be 4 possible materials suitable for the creation of origami-inspired SP designs. These include Mylar (type A), Tyvek, Kapton, and UHMWPE (Ultra-High Molecular Weight Polyethylene).<sup>5</sup> All of the materials were able to undergo 10000+ cycles of fatigue in a custom-designed fatigue tester consisting of a crank-slider mechanism without any tears or holes, making them a suitable choice for this study.<sup>5</sup> However, the chosen material used to recreate the models in the study will be Mylar, a polyester known for its exceptional strength-to-weight ratio. Mylar is a material that is able to withstand harsh environments while having paper-like properties and thickness. It has also been studied that in the Mylar Crease Fatigue Results, the thinner Mylar (177.8  $\mu\text{m}$ ) was able to withstand over 1000+ cycles before failure.<sup>16</sup> The physical property of flexibility is being compared to the materials from which the SCs are made. SCs are made of different materials and alloys, including the most popularly used Silicon (Si), Cu(In,Ga)Se<sub>2</sub>, and CH<sub>3</sub>NH<sub>3</sub>PbI<sub>3</sub>, which are nowadays used for SPs creation.<sup>1</sup> Even though Mylar is not sensitive to environmental changes, it is still significant to keep the environmental factors, such as temperature and humidity, the same during the experimentation process. The Mylar Type-A material is used in many reliable studies for structural integrity testing. For example, Mylar has been utilized as the main material for Kresling origami fold physical testing.<sup>16</sup>

Properties of Mylar relevant for this study include tensile strength, tear strength, elastic constants, and shrinkage. The following qualities for Type-A Mylar can be seen in Table 1.

**Table 1:** Mylar Type-A material characterization was used in the physical testing.<sup>17</sup> Properties of Mylar which are relevant for the physical testing are shown, including tear strength, tensile strength, elastic constraints, and shrinkage.

Tear strength	Tensile strength	Elastic constants	Shrinkage
23.6*10 <sup>6</sup> g/m at 23°	172MPa at 23°	1.6*10 <sup>10</sup> Pa <sup>-1</sup> oriented	2.5%, 30 min at 150°

Potential uncertainties in the physical testing may arise from variations in material properties, inaccuracies in folds,

and human factors during model construction. Assumptions include uniformity in the material properties of Mylar across all models, while limitations may involve the inability to replicate the full range of environmental conditions experienced in space (including other space environment features apart from the external impact, including plasma or solar wind, directly ionizing radiations, thermal cycles, solar activity, and neutral atmosphere with vacuum).<sup>16</sup>

#### *Experimental setup:*

The following paragraph contains information on the experimental setup for mechanical and physical testing on the origami models to determine their structural integrity. The setup involved 15 cm x 10 cm cardboard borderlines, inside of which one model at a time was placed.

The goal is to compare the strength of 2 origami patterns in the fairest way possible.

Below is a step-by-step description of the method to physically test the structural integrity and strength of the origami patterns:

1. Place a folded model vertically on a flat surface inside the fence-like cardboard area
2. Place a weight-distributing platform on top of the model (for equal spread of the pressure and weight onto the mountain creases). Cardboard weight-distributing platform: 11 cm x 6.5 cm.
3. Add weights in increments of 10g onto the cardboard platform
4. Record the maximum weight each fold can withstand before collapsing
5. Repeat for 5 models of each origami pattern type

The weight loads at which each origami model collapses will be recorded, and the mean collapsing weight for each design will be calculated to compare structural performance and determine the strongest pattern. To ensure a fair comparison, weight distribution will be standardized by maintaining consistent contact between the cardboard and the same number of mountain creases on each model.

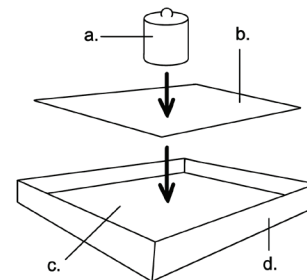


**Figure 9:** The setup for the experiment, where a is the weight load, b is a weight-distributing platform, c is a place where the origami piece will be trapped to undergo a physical test, and d is a cardboard fence to keep the origami model in the same shape.

In Figure 9 above, the setup for the experiment is shown. The only value getting changed is going to be the weights, where they will be added by 10g until the origami collapses.

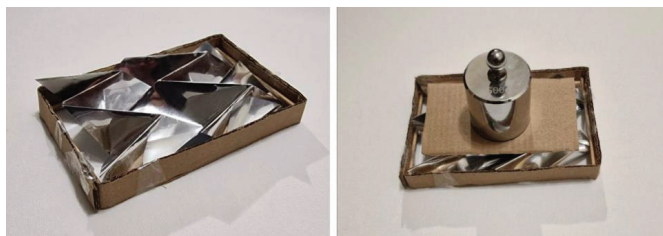


**Figure 10:** The experimental setup images for Miura-Ori showing it in the cardboard fence.

Since 5 models were created for the 2 different origami patterns, the weights were tested on each one until collapse, to then collect the mean for the sample. The mean is a statistical measure of central tendency, defined as the sum of all observed values in a data set divided by the total number of observations. It represents the average value around which the data are distributed. The results for the weight until collapse could be seen in the results and discussions part. The cardboard platform, on which the weights were loaded, was able to cover all four mountain creases in the Miura fold and eight mountain creases in the Flasher fold, as shown in Figure 10. The cardboard outline was used to maintain a specific angle between the cells in the Miura and Flasher folds because the pressure applied may differ depending on the acuteness of this angle. A cardboard platform piece was needed to address the issue of uneven pressure created by the weights, thus spreading the weight force evenly across the creases. It was decided that the experiment would use an acute angle of  $50^\circ$  between the mountain crease vertices for both origami patterns since it is proven to be optimal for both origami folds.<sup>14</sup>

The metallic weights used vary from 10 g to 500 g. Overall, they make up 1 kilogram. The metal-made weights are placed exactly in the middle in each of the tests, making sure the weight is distributed evenly across the cardboard piece at the top.



**Figure 11:** Weights kit including weights of 10g, 20g, 20g, 50g, 100g, 100g, 200g, 500g, totalling 1 kg overall.

The weights used in the experiment are shown above in Figure 11. Added in intervals of 10g, they were placed in the middle piece of cardboard to test the origami structures in terms of their structural strength.

#### ***Comparison and assessment:***

To assess the structural integrity, the maximum load that the origami folding technique can withstand will be measured and compared, and the record of its resistance, deformation, and failure points will be collected. Important factors to assess would also include stress distribution and deformation patterns, which will be recorded and identified by taking pho-

tos. To make the experiment as reliable as possible, five other copies of the origami patterns will be used. By calculating the mean and then comparing the values, the goal of the paper is to determine the most common weight needed to make the origami structure fail.

For the most accurate result, the origami models will be placed with the vertices at the same angles, with both origami patterns having 50-degree mountain creases, so that the pressure affecting the model is the same. To ensure the angles are measured correctly, the protractor has been used. However, there are twice as many mountain creases in the Flasher model, which could create a higher surface area. The difference in surface area would be mostly insignificant due to the mountain creases being extremely small in terms of surface area, so the weight will act almost equally.

## ■ Results

Table 2 represents the data obtained from physical and mechanical tests on the Miura and Flasher origami folds and the weight needed to cause a collapse of the origami structure under the same conditions. The mass in grams was recorded as soon as the origami model collapsed (by collapse, it means the model got compressed under the weight, unable to withstand the pressure). Figure 12 shows the consequences of collapse for both Miura-Ori and Flasher, respectively. As expected, due to Mylar Type-A's properties, the material did not show any signs of tears or stretches; however, the dents were visible as a result of pressure.

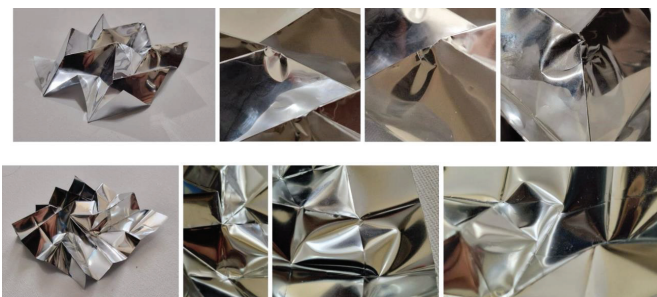


**Figure 12:** Examples of Miura-Ori (row above) and Flasher post collapse (row below).

As a result of physical testing, all of the data have been summarized in Table 2, where the maximum weight until collapse has been recorded for each origami model and its 5 copies. The mean has been calculated for all 5 attempts. The angle in degrees has also been indicated as a reference to show that the optimal angle for both Miura-Ori and Flasher has been kept the same throughout the experimentation.

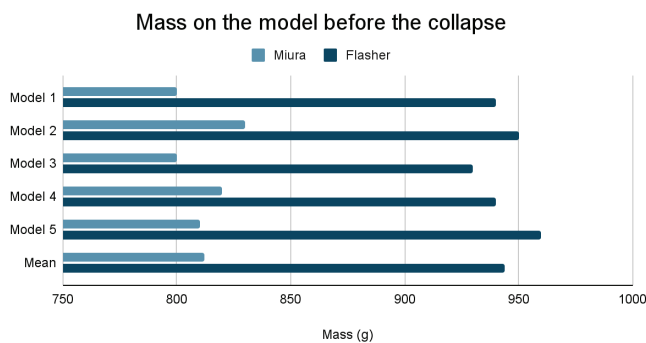
**Table 2:** Results of the physical experiments on the Miura and Flasher models with the mean. The mean weights at which the models collapsed have been recorded for the same optimal angle for both origami types.

Model	Miura 1	Miura 2	Miura 3	Miura 4	Miura 5	mean
Angle between the cells(°)	50	50	50	50	50	50
Max weight until collapse(g)	800	830	800	820	810	812

Model	Flasher 1	Flasher 2	Flasher 3	Flasher 4	Flasher 5	mean
Angle between the cells(°)	50	50	50	50	50	50
Max weight until collapse(g)	940	950	930	940	960	944

The data collected could be represented in a visual and more understandable way by using the bar chart as shown in Figure 13, where the light colour has been used to indicate results for Miura-Ori, and the darker colour has been used to indicate the results for Flasher.



**Figure 13:** Bar chart results showing the mass needed to reach the collapse in Miura-Ori and Flasher models, including their mean mass withstood before the collapse on the x-axis, and the model number with mean on the y-axis.

## Discussion

The Miura origami fold all snapped towards one of the two cell sides, where the highest vertices experienced the most pressure. It is common to observe bending within the cell angles and a dent (visible on the cells from one side), as well as deflection of the obtuse angles on the mountain convex creases. No issues were noticed in the valley concave creases. Interestingly, however, in Miura model 5 and Miura model 4, there was a dent seen in the middle of the parallelogram, which was not observed in the other models. This could be caused by excessive pressure on a specific mountain crease, resulting in one cell bending fully under the weight and disrupting its usual fold pattern.

The Flasher origami fold, however, experienced far less damage compared to the Miura. The damage was usually seen in one of the four clockwise sections, leaving a dent between the folds or resulting in incorrect bend lines for the folds. Like the Miura, the most significant damage was observed at the top of the mountain creases, where the bent creases with the largest dents were located. Interestingly, in Flasher model 2, there is a dent at the very edge of the origami. Similar to the anomaly in the Miura models, it is suggested that this dent could be caused

by excessive pressure on this specific side of the Flasher, leaving its lower part deformed.

With a difference of 132 grams between the mean results for Flasher and Miura, it is evident that the Flasher folding pattern has higher structural integrity and resistance to external impacts. Even looking at Figure 14 is enough to understand that the ability to withstand the weight is drastically different between the two origami pattern folds. The strength and compressibility tests showed that both types of origami patterns have high structural strength; however, Flasher notably demonstrated better results for the SPs compared to the Miura origami technique. Flasher withstood a range of 930-960 grams, outperforming Miura's range of 800-830 grams. By calculating the Miura average as 815g and Flasher as 945g, their difference in averages is equivalent to 130. As a result, it is relevant to note that Flasher was able to outperform Miura-Ori by 16%, all due to its origami fold being more suitable to stand against higher pressure.

The experiment was fair, as both model types used the same acute angle for their dihedral angle (50 degrees), the same deployed area, and the same material, along with its thickness. While some limitations were discussed previously, overall, the experiment was successful in identifying a more robust origami folding technique for the deployment of SPs in space applications for spacecraft.

## Conclusion

In conclusion, the paper's goal of comparing Miura-Ori and Flasher origami patterns concerning the structural integrity of deployable solar panels was to determine which origami type has higher structural integrity. With the physical testing and controlled conditions, both origami model types were tested on their ability to withstand the weight compressing them until the collapse point. Under quasi-static compression, Flasher-patterned 15 cm Mylar panels sustained 16% higher peak load than Miura-Ori equivalents ( $944 \pm 10$  g vs.  $812 \pm 12$  g). The rotational symmetry of Flasher redistributes stress, delaying hinge buckling, making it a more suitable technique for deployable SPs that need better structural integrity for space missions. When translated into real size, even though geometrical similarities will be the same, the material will still differ. Given Mylar's unique similarity to PV cells, it ultimately is still different, and the % of weight with standard could differ from expectations as well. Another limitation of this study is the fact that only 5 models were tested for each; this encourages further research to use even more samples to ensure an even higher credibility. Still, his paper could be valuable for selecting the Flasher as a preferable choice for further spacecraft development for SP usage. Based on the research, it is suggested that similar studies in the future could expand on the topic by comparing Flasher to other origami fold patterns or by exposing it to space environmental stress simulations to further validate Flasher's potential in deployment scenarios.

## ■ Acknowledgments

I would like to express my gratitude to Dr. Bullock and Ms. Long for their invaluable assistance in the process of writing this research paper. The advice and guidance I have received made it key to conduct and finish this research successfully.

## ■ References

- Verduci, R.; Romano, V.; Brunetti, G.; Yaghoobi Nia, N.; Di Carlo, A.; D'Angelo, G.; Ciminelli, C. Solar Energy in Space Applications: Review and Technology Perspectives. *Advanced Energy Materials* 2022, 12 (29), 2200125. <https://doi.org/10.1002/aenm.202200125>.
- Rodgers, E.; Gertsen, E.; Sotudeh, J.; Mullins, C.; Hernandez, A.; Le, H.; Smith, P.; Reviewer, N.; Charania, A.; Colvin, T.; Meyers, R. *Office of Technology, Policy, and Strategy Space-Based Solar Power*, 2024. <https://www.nasa.gov/wp-content/uploads/2024/01/otps-sbsp-report-final-tagged-approved-1-8-24-tagged-v2.pdf?emrc=744da1%0A> (accessed 2025-08-06).
- Yogesh, S.; Yogalakshmi, M.; Abishek, M.; Ari Prasath, R.; Madhusudanan, G. Origami-Based Folding Techniques for Solar Panel Applications. *Int. J. Electr. Eng. Technol.* 2021, 12 (3), 195–203. [https://d1wqtxts1xzle7.cloudfront.net/67663917/IJEEET\\_12\\_03\\_022-libre.pdf](https://d1wqtxts1xzle7.cloudfront.net/67663917/IJEEET_12_03_022-libre.pdf)
- Yue, S. A Review of Origami-Based Deployable Structures in Aerospace Engineering. *Journal of Physics* 2023, 2459 (1), 012137–012137. <https://doi.org/10.1088/1742-6596/2459/1/012137>.
- Morgan, J.; Magleby, S. P.; Howell, L. L. An Approach to Designing Origami-Adapted Aerospace Mechanisms. *Journal of Mechanical Design* 2016, 138 (5). <https://doi.org/10.1115/1.4032973>.
- Garcia, D. J.; Bettinger, R. A.; Hartsfield, C. Simulated Debris Impact Testing of Additively Manufactured Origami Mirror Structure for Space-Based SSA. Poster presented at the Advanced Maui Optical and Space Surveillance Technologies Conference (AMOS), Maui, HI, Sept 2023.
- Huseynli, A. Geometric and Mobility Analysis of the Miura-Ori Pattern and Its Derivations; Master's Thesis, Izmir Institute of Technology, 2016. <https://openaccess.iyte.edu.tr/bitstream/11147/5708/1/T001537.pdf>
- Liu, S.; Lu, G.; Chen, Y.; Leong, Y. W. Deformation of the Miura-ori Patterned Sheet. *Int. J. Mech. Sci.* 2015, 99, 130–142. <https://doi.org/10.1016/j.ijmecsci.2015.05.009>
- Karagiozova, D.; Zhang, J.; Lu, G.; You, Z. Dynamic In-Plane Compression of Miura-Ori Patterned Metamaterials. *Int. J. Impact Eng.* 2019, 129, 80–100. <https://doi.org/10.1016/j.ijimpeng.2019.02.012>
- Demir, D. *A Comprehensive Perspective into the Use of Origami in Architecture*; Abdullah Gül University, 2023.
- Wang, S.; Gao, Y.; Huang, H.; Li, B.; Guo, H.; Liu, R. Design of Deployable Curved-Surface Rigid Origami Flashers. *Mech. Mach. Theory* 2022, 167, 104512. <https://doi.org/10.1016/j.mechmachtheory.2021.104512>
- Srinivas, V.; Harne, R. L. Directing Acoustic Energy by Flasher-Based Origami Inspired Arrays. *The Journal of the Acoustical Society of America* 2020, 148 (5), 2935–2944. <https://doi.org/10.1121/10.0002483>.
- Lu, L.; Leanza, S.; Zhao, R. Origami with Rotational Symmetry: A Review on Their Mechanics and Design. *Applied Mechanics Reviews* 2023, 75 (5). <https://doi.org/10.1115/1.4056637>.
- Chen, Y.; Shi, P.; Bai, Y.; Li, J.; Feng, J.; Pooya Sareh. Engineered Origami Crease Perforations for Optimal Mechanical Performance and Fatigue Life. *Thin-Walled Structures* 2023, 185, 110572–110572. <https://doi.org/10.1016/j.tws.2023.110572>.
- Xiang, X.; Qiang, W.; Hou, B.; Tran, P.; Lu, G. Quasi-Static and Dynamic Mechanical Properties of Miura-Ori Metamaterials. *Thin-Walled Structures* 2020, 157, 106993. <https://doi.org/10.1016/j.tws.2020.106993>.
- Dunne, F.; Westra, K.; Mattox, C.; Leachman, J. Fatigue Life Characterization of Hand Folded and Vacuum Formed Kresling Origami Bellows at 77K. *IOP Conference Series: Materials Science and Engineering* 2022, 1241 (1), 012014. <https://doi.org/10.1088/1757-899x/1241/1/012014>.
- Mark, J. E.; Allcock, H. R.; West, R. Properties of Films Are Given for Mylar Type A (DuPont) Biaxially Oriented and Crystalline Films. In *Polymer Handbook*; Brandrup, J., Immergut, E. H., Grulke, E. A., Eds.; Wiley: New York, 1999; pp 33–46.

## ■ Author

Aruzhan Muratbekova is an open-minded student who is highly interested in music, sciences, and art. Engineering, origami, and architecture are areas of her interest that she would want to explore on a deeper level in university. Being a part of the Haileybury Almaty school, she actively participates in the school life as a house leadership team member and violinist.